Applied Radiation and Isotopes 97 (2015) 52–58

Contents lists available at ScienceDirect

Applied Radiation and Isotopes

journal homepage: www.elsevier.com/locate/apradiso

Cross section measurements of deuteron induced nuclear reactions on natural tungsten up to 34 MeV

C. Duchemin [a,*], A. Guertin [a], F. Haddad [a,b], N. Michel [a,b], V. Métivier [a]

[a] SUBATECH, Ecole des Mines de Nantes, Université de Nantes, CNRS/IN2P3, Nantes, France
[b] GIP Arronax, 1 rue Aronnax, 44817 Saint-Herblain, France

HIGHLIGHTS

- Deuteron induced reactions on natural tungsten up to 34 MeV.
- Experimental values were determined using the stacked-foil technique.
- Comparison with the TALYS code version 1.6.
- Thick target yield of ^{186g}Re, ^{183,182g,184m,184g,181}Re and ^{187}W.

ARTICLE INFO

Article history:
Received 13 June 2014
Received in revised form
4 November 2014
Accepted 9 December 2014
Available online 12 December 2014

Keywords:
Tungsten target
Deuteron beam
Stacked-foil technique
Excitation function
TALYS 1.6

ABSTRACT

^{186g}Re is a β-/γ emitter of great interest for nuclear medicine. It has shown successful results on bone metastases palliation and has similar chemical properties as ^{99m}Tc, the most commonly used imaging agent. ^{186g}Re is routinely produced using rhenium target in nuclear reactor. Higher specific activity could be obtained using accelerators. In this paper, production cross section values are presented for the ^{nat}W$(d, x)^{186g}$Re reaction up to 34 MeV, using the stacked-foils method and gamma spectrometry. From this data set, the thick target production yield of ^{186g}Re is determined and compared with the validated values of the IAEA and also with the proton route. The production cross sections of the ^{nat}W$(d, x)^{183,182g,184m,184g,181}$Re and ^{nat}W$(d, x)^{187}$W reactions have also been determined. A good agreement is found with the literature. Our data are compared with the version 1.6 (December 2013) of the TALYS code which shows discrepancies both on the shape and on the amplitude for these deuteron induced reactions.

1. Introduction

In the field of medical radioisotope production, the knowledge of the activation cross section allows to quantify and control the production of a radionuclide. ^{186g}Re ($T_{1/2}$=3.7 days), is a β- emitter which has been used in clinical trials for palliation of painful bone metastases resulting from prostate and breast cancer (Palmedo et al., 2001). This radionuclide is currently produced with nuclear reactor using ^{185}Re enriched target or aluminum perrhenate target (Ishfaq et al., 1999; Ehrhardt et al., 1997; Knapp et al., 1997; Ehrhardt et al., 1996). These production routes lead to a low specific activity. To obtain high specific activity product, ^{186g}Re could be advantageously produced on a tungsten target with cyclotrons able to accelerate deuterons or protons (Guertin et al., 2014). This paper reports activation cross section values and thick target production yields for the ^{nat}W$(d, x)^{186g,184m,184g,183,182g,181}$Re and ^{nat}W$(d, x)^{187}$W reactions up to 34 MeV. These data are compared with the literature and the TALYS code calculations (Koning and Rochman, 2012). This large set of data is of interest for the International Fusion Materials Irradiation Facility project (IFMIF) in the estimation of the deuteron-activation of structural materials (Gobin et al., 2009) and could help to constrain theoretical codes on cross section predictions.

2. Materials and methods

2.1. Experimental set-up

Cross section measurements are made using the stacked-foils method (Blessing et al. (1995); Duchemin et al., 2014; Guertin et al., 2014). A set of thin foils is irradiated containing 10 μm thick tungsten targets, 10 μm thick titanium monitor foils to have

* Corresponding author.
E-mail address: Charlotte.Duchemin@subatech.in2p3.fr (C. Duchemin).

http://dx.doi.org/10.1016/j.apradiso.2014.12.011
0969-8043/

Table 1
Irradiation conditions.

Beam energy (MeV)	⟨Intensity⟩ (nA)	Energy points (MeV)				
34.00 (25)	206	33.36 (30)	32.13 (35)	27.91 (49)	23.11 (59)	20.93 (63)
30.75 (25)	141	30.06 (29)	26.35 (41)	24.39 (46)	19.85 (58)	18.43 (64)
16.90 (25)	113	14.67 (38)	13.32 (43)	11.85 (50)	10.42 (56)	8.85 (66)
30.75 (25)	105	22.37 (55)				
22.59 (25)	101	16.96 (31)				
16.90 (25)	82	15.52 (33)	12.87 (44)	9.74 (57)		

informations on the beam flux and thick aluminium degrader foils (between 100 and 500 μm) to change the incident beam energy, which impinged the tungsten foils.

The ARRONAX cyclotron delivers a deuteron beam with an energy within ± 0.25 MeV (Haddad et al., 2008). All along the stack, depending on the number of foils, the energy uncertainty calculated using the SRIM software (Ziegler et al., 2010) increases up to ± 0.7 MeV due to the energy straggling. Several stacks were irradiated with a different incident energy in order to minimize this energy dispersion and cover the full energy range from 34 MeV down to the reaction thresholds. This way, we were also able to overlap data points and be sure that our experiments are under control. Typical irradiations were carried out with a beam intensities between 80 and 200 nA for 30 min. Irradiation conditions are reported in Table 1.

The stacks were irradiated with an external deuteron beam, delivered by the ARRONAX cyclotron. A 75 μm thick kapton foil closes the line and makes a barrier between the air in the vault and the vacuum in the beam line. The stacks were located about 7 cm downstream in air. The energy through each thin foil was determined in the middle of the thickness of the foil using the SRIM software (Ziegler et al., 2010). Energy loss in the kapton foil and air were taken into account.

All foils were purchased from Goodfellow® with high purity (>99.6%). The natural isotopic compositions of the foils are reported in Table 2. Each thin foil has been weighed before irradiation using an accurate scale ($\pm 10^{-5}$ g) and scanned to precisely determine their area. From these values and assuming that the thickness is homogeneous over the whole surface, the thickness is deduced. A Faraday cup was placed after the stack to collect charges and control the intensity during the irradiation. Titanium monitor foils have been placed behind each target foil, to record the particle flux all along the stack through the ^{nat}Ti(d, x)^{48}V reaction as recommended by the IAEA (Tárkányi et al., 2001).

The activity measurements in each target and monitor foils were performed using a high purity germanium detector from Canberra (France) with low-background lead and copper shielding. All foils were counted twice: starting the day after the irradiation (for few hours) and after 2 or 3 weeks (for more than 48 h). Gamma spectra were recorded in a suitable geometry calibrated in energy and efficiency with standard ^{57,60}Co and ^{152}Eu gamma sources from LEA-CERCA (France). Samples were placed at a distance of 19 cm from the detector in order to reduce the dead time and pile-up. The dead time during the counting was always below 10%.

Table 2
Isotopic composition of natural Ti and W foils from Goodfellow®.

^{46}Ti	^{47}Ti	^{48}Ti	^{49}Ti	^{50}Ti
8.0 %	7.5 %	73.7 %	5.5 %	5.3 %
^{180}W	^{182}W	^{183}W	^{184}W	^{186}W
0.1 %	26.3 %	14.3 %	30.7 %	28.6 %

2.2. Data processing

The activity values of the produced radioisotopes were derived from the γ spectra and the nuclear decay data given in Table 3, using the Fitzpeak spectroscopy software (FitzPeaks Gamma Analysis and Calibration Software Version 3.66, 1981). Knowing the precise thickness of the foil and the activity value of the produced isotope, its cross section is calculated using the well-known activation formula (Duchemin et al., 2014; Guertin et al., 2014). The chemical purity of the sample was taking into account: 99.95% for W and 99.6% for Ti.

As each target is followed by a titanium monitor foil, which receive the same deuteron flux, the cross section is deduced with a relative calculation using the recommended ^{nat}Ti(d, x)^{48}V cross section. The ^{48}V activity was extracted using the γ lines at 944.13, 983.525 and 1312.106 keV (Ekström and Firestone, 2004). The uncertainty on the production cross section is calculated as a quadratic form (Duchemin et al., 2014; Guertin et al., 2014). Main errors come from the measured activity (from 5 to 40% in W target and up to 2% for ^{48}V), the thickness of the foils (around 1%) and the uncertainty on the ^{48}V recommended cross section (around 12%). The contribution of the irradiation time is not significant and has been neglected.

Table 3
Produced radioisotope parameters (National Nuclear Data Center, Ekström and Firestone, 2004).

Radioisotope	$T_{1/2}$	E_γ(keV)	I_γ (%)
^{181}Re	19.9 (7) h	365.570	56 (6)
		953.420	3.6 (9)
		639.30	6.4 (13)
^{182g}Re	64.0 (5) h	130.80	7.5 (5)
		169.151	11.3 (8)
		191.380	6.7 (5)
		256.450	9.5 (8)
		276.311	8.7 (5)
		286.554	7.0 (5)
		339.060	5.6 (4)
		351.070	10.3 (8)
		1076.30	10.5 (3)
		1427.00	9.79 (18)
^{183}Re	70.0 (11) d	162.322	23.30 (40)
		208.8057	2.95 (5)
		291.724	3.05 (16)
^{184g}Re	38.0 (5) d	792.07	37.5 (6)
		894.757	15.6 (3)
		903.28	37.9 (6)
^{184m}Re	169 (8) d	104.729	13.40 (40)
		318.012	5.75 (8)
		920.932	8.14 (12)
^{186g}Re	3.7183 (11) d	137.157	9.42 (6)
^{187}W	23.72 (6) h	479.531	21.8 (4)
		551.532	5.08 (11)
		618.361	6.28 (14)
		685.774	27.3 (6)
		772.890	4.12 (8)

2.3. Comparison with the TALYS 1.6 code

TALYS is a nuclear reaction program to simulate reaction induced by light particles on nuclei heavier than carbon. It incorporates many theoretical models to predict physical parameters including theoretical cross section values as a function of the incident particle energy (from 1 keV to 1 GeV). In this work, all the experimental cross section values are compared with the last version (1.6) of the TALYS code (december, 2013), with default parameters (Koning and Rochman, 2012).

3. Results

Our activation cross section results for the $^{nat}W(d, x)^{186g}Re$ reaction are presented in this section, as well as those of the other radionuclides produced in our target, and detectable by our device, which are of interest in the specific activity determination. No fission products or tantalum radioisotopes have been detected, as they are under the detection limit of our device. These data are plotted as full circles in Figs. 1–7 and compared with the published experimental values (EXFOR database, National Nuclear Data Center), and with the results obtained with the TALYS code. The numerical values are reported in Table 5. The thick target yields of the $^{nat}W(d, x)^{186g,183,182g,184m,184g,181}Re$ and $^{nat}W(d, x)^{187}W$ reactions are presented at the end of this paper.

3.1. Production of ^{186g}Re

^{186g}Re has a half-life of 3.7183 days and decays at 92.53% by β- to ^{186}Os (stable) and at 7.47% by EC to ^{186}W (stable). Its gamma line, $E_\gamma = 137.157$ keV ($I_\gamma = 9.42\,(6)\,\%$), coming from the β- decay, is used to measure the activity (see Table 3). We supposed that the metastable state ^{186m}Re contribution is negligeable due to its very long half-life (2.10^5 years) compared with our experiment duration. ^{186g}Re can only come from the ^{186}W (with an isotopic abundance of 28.6%), via the reaction $^{186}W(d, 2n)^{186g}Re$. It is then possible to extract, from our data, the production of ^{186g}Re considering an enriched target. Our data set is presented in Fig. 1 with others results previously published, the values recommended by the IAEA (Tárkányi et al., 2003) and the version 1.6 of the TALYS code. Our results are very close to Zhenlan et al. (1981), in the range 7–12 MeV. Tárkányi et al. (2003) and Ishioka et al. (2002) have contributed with higher energy beams. Our results are in good agreement, especially with Tárkányi et al. (2003). The results of Ishioka et al. (2002) are higher than ours. The TALYS code does not give satisfactory results, especially on the amplitude.

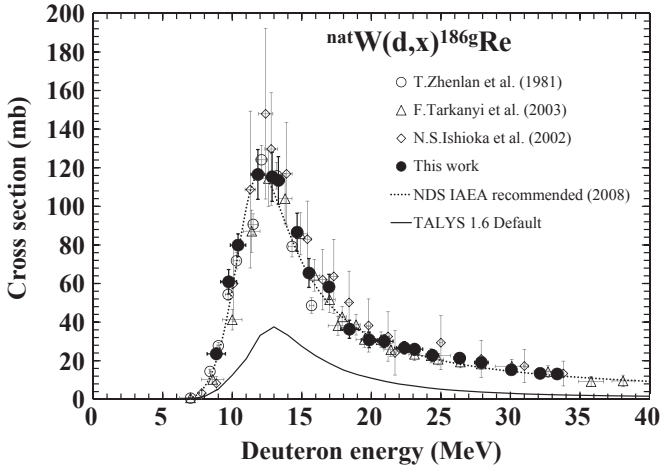

Fig. 1. $^{nat}W(d, x)^{186g}Re$ production cross section.

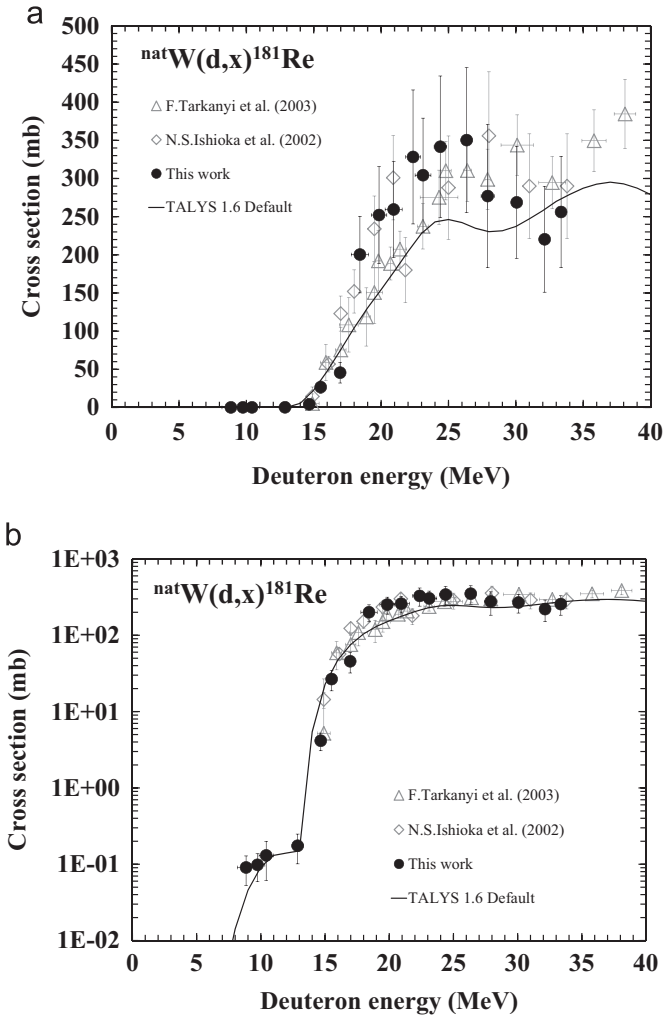

Fig. 2. $^{nat}W(d, x)^{181}Re$ production cross section. Linear scale (a) and logarithmic scale (b).

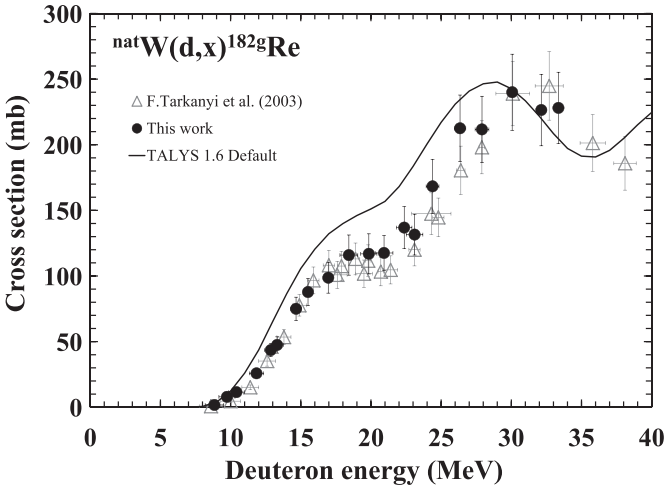

Fig. 3. $^{nat}W(d, x)^{182g}Re$ production cross section.

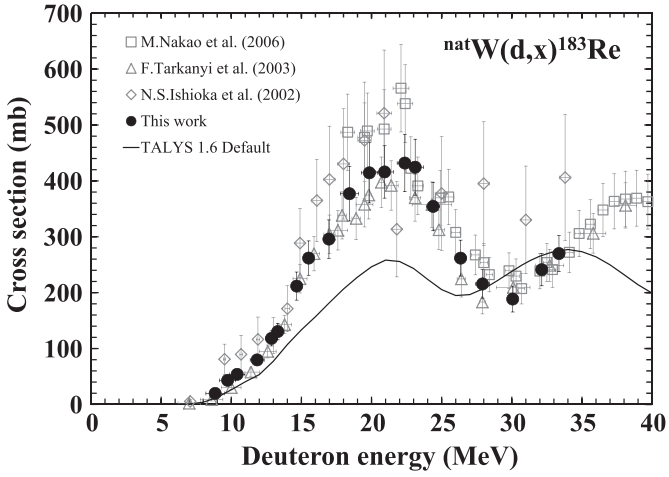

Fig. 4. $^{nat}W(d, x)^{183}Re$ production cross section.

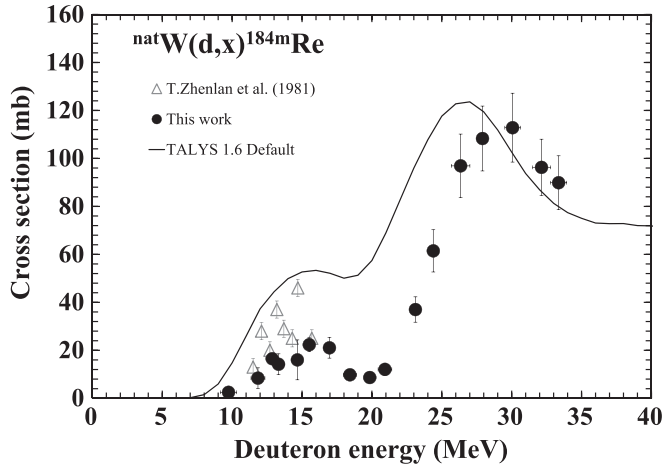

Fig. 5. $^{nat}W(d, x)^{184m}Re$ production cross section.

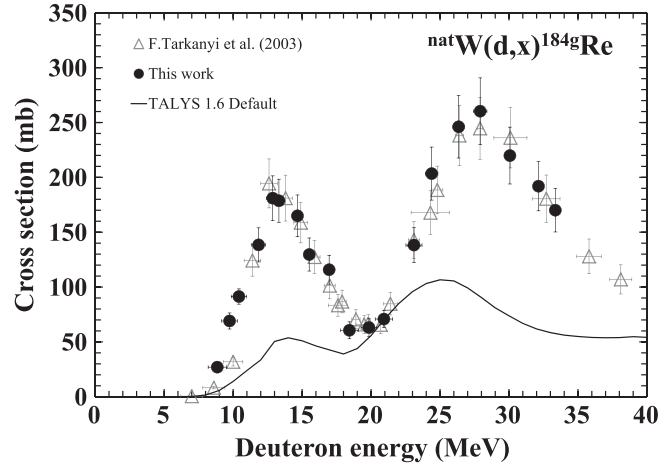

Fig. 6. $^{nat}W(d, x)^{184g}Re$ production cross section.

3.2. Production of ^{181}Re

^{181}Re has a half life of 19.9 h and decays by electron capture (EC) to ^{181}W ($T_{1/2}$=121 days). Its gamma line at 365.570 keV (I_γ = 56 (6) %) was used to determined the activity. Two others gamma lines with lower branching ratio (reported in Table 3), identified in the spectrum, lead to comparable activities. ^{181}Re

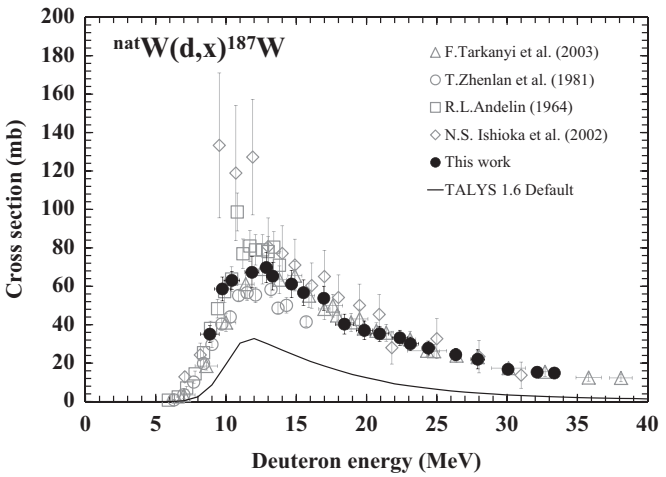

Fig. 7. $^{nat}W(d, x)^{187}W$ production cross section.

experimental cross section is plotted in Fig. 2 with a linear scale (a) and a logarithmic scale (b). Logarithmic scale allows to show the contribution of the ^{180}W (d, n) reaction between 0 and 12 MeV. This tungsten isotope has a very low isotopic abundance (0.1%), which explains the small contribution to the cross section. The linear scale lets appreciate the maximum of the cross section at 26 MeV with 350 mb. Looking at the contributing reactions in Table 4, this maximum is mainly due to the reactions on the ^{182}W and ^{183}W isotopes. Our values can be compared with Tárkányi et al. (2003) and Ishioka et al. (2002). They are in agreement taking into account the uncertainty bars. These errors are mainly due to the 11% of uncertainty on the gamma line used to determine the activity. The TALYS 1.6 code gives results close to the experimental values.

3.3. Production of ^{182g}Re

^{182g}Re, with a half life of 64 h, emits several gamma lines between 130 and 1427 keV (see Table 3), which are not common with its metastable state. ^{182m}Re does not feed the ground state. The activity extracted from each of this gamma lines was in total agreement giving us confidence in our values. Our $^{nat}W(d, xn)^{182g}Re$ production cross section values are plotted in Fig. 3 and compared with the work of Tárkányi et al., (2003). ^{182g}Re can be produced on four of the five isotopes constituting the

Table 4
Contributing reactions and threshold (National Nuclear Data Center).

Radioisotope	Contributing reaction(s)	$E_{threshold}$ (MeV)
^{181}Re	^{180}W (d, n)	0.00
^{182g}Re	$^{182}W(d, 2n)$	5.87
	^{183}W (d, $3n$)	12.13
	^{184}W (d, $4n$)	19.62
	^{186}W (d, $6n$)	32.71
^{183}Re	^{182}W (d, n)	0.00
	$^{183}W(d, 2n)$	3.60
	^{184}W (d, $3n$)	11.09
	^{186}W (d, $5n$)	24.18
^{184g}Re	^{183}W (d, n)	0.00
	$^{184}W(d, 2n)$	4.54
	^{186}W (d, $4n$)	17.62
^{184m}Re	^{183}W (d, n)	0.00
	$^{184}W(d, 2n)$	4.54
	^{186}W (d, $4n$)	17.62
^{186}Re	$^{186}W(d, 2n)$	3.63
^{187}W	^{186}W (d, p)	0.00

Table 5
Experimental cross section values (mb) for $^{nat}W(d, x)^{186g,183,182g,184m,184g,181}Re$ and ^{187}W reactions.

Energy (MeV)	σ ^{186g}Re (mb)	σ ^{183}Re (mb)	σ ^{182g}Re (mb)	σ ^{184m}Re (mb)
8.85 ± 0.66	23.56 ± 2.96	19.71 ± 3.11	1.71 ± 0.24	
9.74 ± 0.57	60.90 ± 6.33	43.17 ± 4.61	7.91 ± 0.85	2.50 ± 0.47
10.42 ± 0.56	79.89 ± 5.87	53.77 ± 4.67	11.49 ± 0.94	
11.85 ± 0.50	116.51 ± 12.92	79.68 ± 9.31	25.83 ± 3.04	8.41 ± 4.31
12.87 ± 0.44	115.29 ± 12.75	118.12 ± 13.42	43.52 ± 4.94	16.50 ± 2.13
13.32 ± 0.43	113.42 ± 12.32	130.35 ± 14.75	47.44 ± 6.22	14.20 ± 4.34
14.67 ± 0.38	86.59 ± 9.89	211.68 ± 25.16	74.99 ± 8.87	16.03 ± 8.31
15.52 ± 0.33	65.47 ± 7.50	261.83 ± 30.73	87.73 ± 10.32	22.35 ± 2.88
16.96 ± 0.31	58.24 ± 6.54	295.79 ± 34.33	98.64 ± 11.72	21.06 ± 4.34
18.43 ± 0.64	36.30 ± 4.68	376.98 ± 48.81	115.92 ± 15.32	9.80 ± 2.03
19.85 ± 0.58	30.78 ± 4.02	414.37 ± 53.82	116.87 ± 15.28	8.67 ± 2.23
20.93 ± 0.63	30.04 ± 3.33	415.95 ± 46.85	117.55 ± 13.28	12.05 ± 2.60
22.37 ± 0.55	26.70 ± 3.19	431.84 ± 51.13	136.85 ± 16.02	
23.11 ± 0.59	25.95 ± 2.98	424.43 ± 50.06	131.51 ± 15.51	37.00 ± 5.30
24.39 ± 0.46	22.81 ± 2.94	354.27 ± 43.15	168.30 ± 20.55	61.47 ± 8.80
26.35 ± 0.41	21.34 ± 2.67	261.75 ± 32.16	212.54 ± 25.31	96.90 ± 13.24
27.91 ± 0.49	19.07 ± 2.25	215.60 ± 25.42	211.65 ± 25.26	108.31 ± 13.52
30.06 ± 0.29	15.29 ± 1.88	188.56 ± 23.19	239.99 ± 28.99	112.82 ± 14.35
32.13 ± 0.35	13.46 ± 1.67	241.05 ± 28.84	226.45 ± 27.22	96.28 ± 11.73
33.36 ± 0.30	13.13 ± 1.64	269.91 ± 32.11	228.05 ± 27.19	89.87 ± 11.22
Energy (MeV)	σ ^{184g}Re (mb)	σ ^{181}Re (mb)		σ ^{187}W (mb)
8.85 ± 0.66	26.97 ± 3.48	0.09 ± 0.04		35.10 ± 4.41
9.74 ± 0.57	69.09 ± 7.33	0.10 ± 0.04		58.60 ± 6.0
10.42 ± 0.56	91.36 ± 6.97	0.13 ± 0.07		63.07 ± 4.73
11.85 ± 0.50	138.45 ± 15.55			12.87 ± 0.43
12.87 ± 0.44	181.02 ± 20.37	0.17 ± 0.07		69.76 ± 7.84
13.32 ± 0.43	178.67 ± 19.66			65.28 ± 7.21
14.67 ± 0.38	164.93 ± 19.04	4.15 ± 1.08		61.17 ± 7.06
15.52 ± 0.33	129.66 ± 15.08	26.66 ± 7.94		56.69 ± 6.64
16.96 ± 0.31	115.80 ± 13.19	45.60 ± 13.58		53.78 ± 6.26
18.43 ± 0.64	60.59 ± 7.71	200.33 ± 50.16		40.30 ± 5.17
19.85 ± 0.58	63.04 ± 8.05	252.12 ± 63.40		37.07 ± 4.79
20.93 ± 0.63	70.82 ± 7.78	259.40 ± 62.80		35.26 ± 3.91
22.37 ± 0.55		328.27 ± 87.77		33.17 ± 3.94
23.11 ± 0.59	138.26 ± 15.94	304.32 ± 74.72		30.07 ± 3.46
24.39 ± 0.46	203.43 ± 24.19	341.61 ± 92.70		27.85 ± 3.60
26.35 ± 0.41	246.10 ± 28.50	350.30 ± 94.91		24.38 ± 3.20
27.91 ± 0.49	260.34 ± 30.37	276.96 ± 93.77		22.01 ± 5.00
30.06 ± 0.29	219.86 ± 25.92	268.76 ± 73.30		16.80 ± 2.12
32.13 ± 0.35	191.94 ± 22.45	220.30 ± 69.32		15.28 ± 2.75
33.36 ± 0.30	170.04 ± 19.84	256.14 ± 72.95		14.85 ± 1.91

natural tungsten target. These reaction channels, with threshold values reported in Table 4, can be easily identified on the experimental activation cross section trend. Compared to Tárkányi et al. (2003), our results are in good agreement but with values slightly higher between 20 and 28 MeV. The TALYS code pretty well reproduced the trend and the different reaction channels but overestimate the cross section up to 30 % in some cases.

3.4. Production of ^{183}Re

The decay of ^{183}Re is accompanied by three main gamma radiations presented in Table 3. It can be produced on the same tungsten isotopes as ^{182g}Re, previously presented. Our results are plotted in Fig. 4 with three other data sets. These data show that the maximum cross section is around 22 MeV but with a different magnitude depending on the series. Our new values are similar to those of Tárkányi et al. (2003) and are in agreement with Nakao et al. (2006) only between 23 and 33 MeV. Significant differences with Ishioka et al. (2002) are observed on the whole energy range. The TALYS code gives a good trend up to 25 MeV even if the magnitude is underestimated. However, from this point, the cross section seems to be shifted towards lower energies.

3.5. Production of ^{184m}Re and ^{184g}Re

^{184m}Re, with a half life of 169 days, decays by IT (74.5%) to the ground state ^{184g}Re and by EC (25.5%) to ^{184}W. Three γ lines summarized in Table 3 permit to extract the ^{184m}Re activity. ^{184m}Re production cross section is plotted in Fig. 5 with the results of Zhenlan et al. (1981). The comparison can be made only up to 15 MeV, because no experimental data have been already published above this energy. Our results are always below the data of Zhenlan et al. (1981). From 15 MeV, our new experimental data set has the same shape as TALYS.

^{184g}Re, with a half life of 38 days, decays by EC (100%) to ^{184}W. We have previously seen that ^{184g}Re is fed by ^{184m}Re. As both states have some γ lines in common but also different ones, we were able to extract the activity of ^{184g}Re without the direct production contribution of ^{184m}Re. The activity values retrieved from the three γ lines summarized in Table 3 were in total agreement. The contribution coming from the decay of ^{184m}Re strongly depends of the measuring time. In our experiments, the gamma spectra are recorded the day after the irradiation for few hours and again several days after the irradiation for more than 24 h in order to get lower uncertainties on the long half-life radionuclides. In the case of ^{184g}Re, we used the second counting to extract the cross section values. The contribution of ^{184m}Re is up to 2.9 % of the total ^{184g}Re

activity and has been subtracted. The independent excitation function of ^{184g}Re is plotted in Fig. 6 with Tárkányi et al. (2003) results. In this latter publication, the authors assume a maximum of 0.2% of ^{184m}Re contribution. Both experiments are in good agreement. Additional data points have been measured for the lower energy part in our experiment. The TALYS code gives a shifted trend compared to the experimental results, as observed for ^{183}Re and ^{184m}Re, and the amplitude is not reproduced.

3.6. Production of ^{187}W

^{187}W is the only tungsten radioisotope we were able to measure. The others tungsten isotopes may be produced but their gamma lines have too low branching ratio (less than 0.09%) to be detected by our experimental tools.

^{187}W with a half life of 23.72 h decreases at 100% by β- to ^{187}Re (stable). It can be detected with different γ lines (see Table 3) with branching ratio higher than 4%, which result in a small uncertainty on the cross section determination. Our results are plotted in Fig. 7 with previous data. Up to 10.5 MeV, our results perfectly follow the Andelin et al. (1964) values. From 11 MeV, our data set is totally in agreement with Tárkányi et al. (2003). In comparison with the other data, the maximum of the curve is different depending on the series. Indeed, around 12 MeV, our values are 13% lower than Andelin et al. (1964), between 14 and 40% lower than Ishioka et al. (2002) and 15% higher than Zhenlan et al. (1981). The TALYS code underestimates by 50 % the amplitude.

3.7. Thick target yield (TTY)

Using the cross section values obtained in this work, we have calculated for each radionuclide produced. Their thick target yield (TTY) in Bq/μA h as a function of the projectile energy, using the following relation:

$$TTY = \Phi\cdot\chi\cdot\frac{N_a\cdot\rho}{A}(1-e^{-\lambda\cdot t})\int_{E_{min}}^{E_{max}}\frac{\sigma(E)}{\frac{dE}{dx}}\,dE \quad (1)$$

where χ is the target enrichment and dE/dx is the specific energy loss of the projectile in the target material (MeV cm^{-1}). In a thick target, the incident particle energy decreases with the penetration depth. E_{max} corresponds to the incident projectile energy when it enters into the target whereas E_{min} corresponds to its energy when it leaves the target. It can also be called production yield or integral yield. The TTY of the different radionuclides produced in the ^{nat}W are plotted in Fig. 8 and reported in Table 6 for the maximum energy 33.4 MeV.

3.7.1. ^{186g}Re production on a natural tungsten target

The IAEA estimates that the integral yield of ^{nat}W$(d,x)^{186g}$Re (Tárkányi et al., 2003) is 7.5 MBq/μA h at 33 MeV against 8.5 MBq/μA h with our experimental values (Fig. 9). This difference can be accounted to the IAEA recommended cross section fit (plotted in Fig. 1), which draw a peak slightly thinner and lower than our points. Other authors have calculated the ^{186g}Re thick target yield since the IAEA recommendation. Hermanne et al. (2009), obtained values in agreement with the recommended thick target yield of the IAEA whereas Bonardi et al. (2010) published data up to 30 % higher. With protons, the recommended integral yield published by the IAEA (Tárkányi et al., 2003) is 2.7 MBq/μA h at 33 MeV (Fig. 9). The deuteron production route is clearly the best choice for the production of this medical radioisotope.

3.7.2. ^{186g}Re production on an enriched tungsten target

For medical applications, the production of contaminants has to be avoided. An easy way to produce ^{186g}Re without contaminants is to use a 100% enriched ^{186}W target irradiated with deuteron beams. When using this tungsten isotope as target, only the ^{186g}Re and ^{184m,g}Re could be produced. With a deuteron energy just below the ^{186}W$(d,4n)^{184m,g}$Re reaction threshold, 17.6 MeV (Table 4), the ^{186g}Re specific activity will be the greatest possible with a TTY of 16.8 MBq/μA h to be compared with the IAEA recommended value of 15.4 MBq/μA h with deuterons and 4.6 MBq/μA h with a proton beam at the same energy.

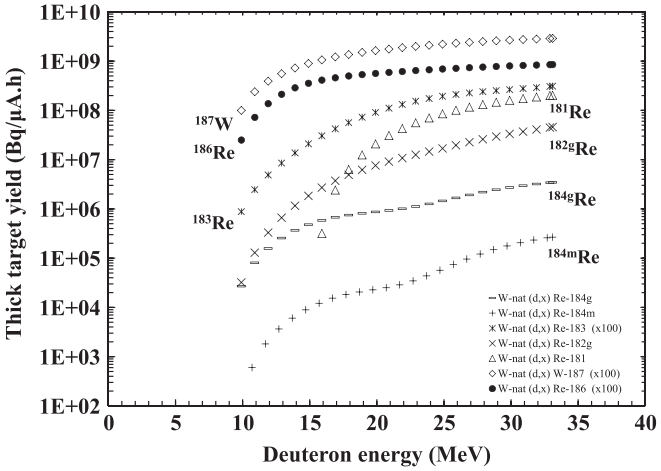

Fig. 8. Thick target yield of the produced radionuclides on ^{nat}W in Bq/μA h.

Table 6
Thick-target yield (TTY) of the different produced radionuclides at 33.4 MeV.

Radionuclide	TTY (MBq/μA h)
^{181}Re	203.2
^{182g}Re	45.7
^{183}Re	3.1
^{184g}Re	3.5
^{184m}Re	0.3
^{186g}Re	8.5
^{187}W	28.8

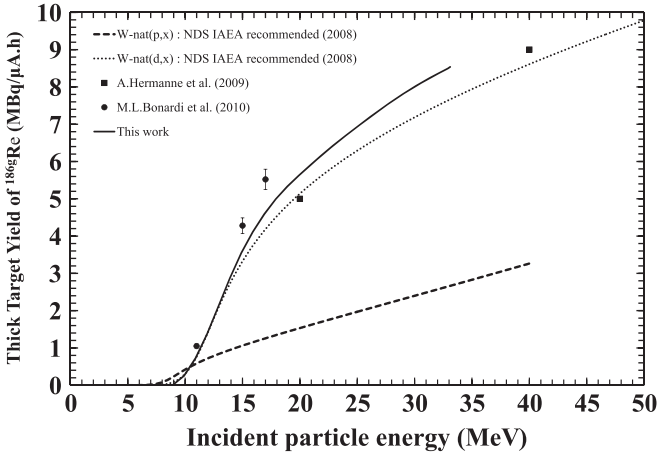

Fig. 9. Comparison of the thick target yields of ^{186g}Re in MBq/μA h.

4. Conclusion

In this paper are presented experimental cross section values for the ^{nat}W$(d,x)^{186g,184m,184g,183,182g,181}$Re and ^{nat}W$(d,x)^{187}$W

reactions, up to 34 MeV. Comparison with previous data sets show that our results are in good agreement with Tárkányi et al. (2003). This study presents for the first time the experimental $^{nat}W(d, x)^{184m}Re$ production cross section above 15 MeV. The thick target yields of all the produced radionuclides are shown. For the medical radioisotope ^{186g}Re, the yields show a production three times higher using deuteron as compared to proton as projectile. For these deuteron induced reactions, a comparison with the TALYS code (version 1.6) has been made with default parameters. It shows discrepancies both on the amplitude and on the shape. Additional data using deuterons on other targets are needed to better constrain the nuclear models.

Acknowledgments

The ARRONAX cyclotron is a project promoted by the Regional Council of Pays de la Loire financed by local authorities, the French government and the European Union. This work has been, in part, supported by a Grant from the French National Agency for Research called “Investissements d'Avenir”, Equipex Arronax-Plus no. ANR-11-EQPX-0004 and Labex no. ANR-11-LABX-0018-01.

References

Andelin, R.L., 1964. Excitation functions for the $^{184}W(d,p)$ ^{185}W, $^{186}W(d,p)$ ^{187}W and $^{184}W(d,2n)$ ^{184}Re reactions; and half-lives of ^{185}W and ^{187}W. J. Inorg. Nucl. Chem. 26 (6), 1117–1120.

Blessing, G., Bräutigam, W., Böge, H.G., Gad, N., Scholten, B., Qaim, S.M., 1995. Internal irradiation system for excitation function measurement via the stacked-foil technique. Appl. Radiat. Isot. 955, 46–49.

Bonardi, M.L., Groppi, F., Manenti, S., Persico, E., Gini, L., 2010. Production study of high specific activity NCA Re-186g by proton and deuteron cyclotron irradiation. Appl. Radiat. Isot. 68, 1595–1601.

Duchemin, C., Guertin, A., Haddad, F., Michel, N., Métivier, V., 2014. $^{232}Th(d,4n)^{230}Pa$ Cross Section Measurements at ARRONAX facility for the production of ^{230}U. Nucl. Med. Biol. 41 (Supplement), e19–e22 http://dx.doi.org/10.1016/j.nucmedbio.2013.12.011.

Ehrhardt, G.J., Blumer, M.E., Su, F.M., Vanderheyden, J.L., Fritzberg, A.R., 1996. Experience with aluminium perrhenate targets for reactor production of high specific activity Re-186. Appl. Radiat. Isot. 48-1, 1–4.

Ehrhardt, G.J., Ketring, A.R., Ayers, L.M., 1997. Reactor-produced radionuclides at the University of Missouri research Reactor. Appl. Radiat. Isot. 49-4, 295–297.

Ekström, L.F., Firestone, R.B., 2004. Information Extracted from the Table of Radioactive Isotopes, Version 2.1.

FitzPeaks Gamma Analysis and Calibration Software Version 3.66, produced by JF Computing Services (UK), based on methods presented in Nucl. Instrum. and Methods (1981) 190, 89–99, describing the program SAMPO80 of the Helsinki University of Technology, Finland.

Gobin, R., et al., 2009. General Design of the IFMIF Deuteron Injector: Source and Beam Line. In: Proceedings of the ICIS09, Gatlinburg Tennessee, USA.

Guertin, A., Duchemin, C., Haddad, F., Michel, N., Métivier, V., 2014. Measurements of ^{186}Re production cross section induced by deuterons on ^{nat}W target at ARRONAX facility. Nucl. Med. Biol. 41 (Supplement), e16–e18 http://dx.doi.org/10.1016/j.nucmedbio.2013.11.003.

Haddad, F., Ferrer, L., Guertin, A., Carlier, T., Michel, N., Barbet, J., Chatal, J.F., 2008. Arronax a high-energy and high-intensity cyclotron for nuclear medicine. Eur. J. Nucl. Med. Mol. Imaging 35, 1377–1387.

Hermanne, A., Daraban, L., Tárkányi, F., Takács, S., Ditrói, F., Ignatyuk, A., Adam Rebeles, R., Bada, M., 2009. Excitations functions for some W, Ta and Hf radionuclides obtained by deuteron irradiation of ^{181}Ta up to 40 MeV. Nucl. Instrum. Methods Phys. Res. B 267, 3293–3301.

Ishfaq, M.M., Mushtaq, A., Jawaid, M., 1999. Experience on the neutron activation of natural/enriched Re, Sm, and Ho nuclides in a reactor for the production of radiotherapeutic radionuclides. Biol. Trace Elem. Res. 71-2, 519–526.

Ishioka, N.S., Watanabe, S., Osa, A., Koizumi, M., Matsuoka, H., Sekine, T., 2002. Excitation functions of rhenium isotopes on the $^{nat}W(d, xn)$ reactions and production of no-carrier-addied ^{186}Re. J. Nucl. Sci. Technol Suppl. 2, 1334–1337.

Knapp Jr., F.F.R.U.S.S., Mirzadeh, S., Beets, A.L., O'Doherty, M., Blower, P.J., Verdera, E. S., Gaudiano, J.S., Kropp, J., Guhlke, J., Palmedo, H., Biersack, H.J., 1997. Reactor-produced radioisotopes from ORNL for Bone Pain Pallation. Appl. Radiat. Isot. 49-4, 309–315.

Koning, A.J., Rochman, D., 2012. Modern nuclear data evaluation with the TALYS code system. Nucl. Data Sheets 113, 2841.

Nakao, M., Hori, J., Ochiai, K., Kubota, N., Sato, S., Yamauchi, M., Ishioka, N.S., Nishitani, T., 2006. Measurements of deuteron-induced activation cross-sections for IFMIF accelerator structural materials. Nucl. Instrum. Methods Phys. Res., Sect. A 562, 785.

National Nuclear Data Center, Information Extracted from the NuDat2 Database. ⟨http://www.nndc.bnl.gov/nudat2/⟩.

Palmedo, H., Rockstroh, J.K., Bangard, M., Schliefer, K., Risse, J., Menzel, C., Biersack, H.J., 2001. Painful multifocal arthritis: therapy with Rhenium 186 Hydroxyethylidenedi-Phosphonate (^{186}Re HEDP) after failed treatment with medication-initial results of a prospective study. Radiology 221, 256–260.

Tárkányi, F., Takács, S., Gul, K., Hermanne, A., Mustafa, M.G., Nortier, M., Oblozinsky, P., Qaim, S.M., Scholten, B., Shubin, Yu.N., Youxiang, Z., 2001. Beam monitor reactions. In: Charged Particle Cross Section Database for Medical Radioisotope Production: Diagnostic Radioisotopes and Monitor Reactions. IAEA-TECDOC-1211, pp. 49–152, IAEA, Vienna. Database available on ⟨https://www-nds.iaea.org/medportal/⟩. Update May 2013.

Tárkányi, F., Takács, S., Szelecsenyi, F., Ditroi, F., Hermanne, A., Sonck, M., 2003. Excitation functions of deuteron induced nuclear reactions on natural tungsten up to 50 MeV. Nucl. Instrum. Methods Phys. Res., Sect. B 211, 319–330.

Zhenlan, T., Fuying, Z., Huiyuan, Q., Gongqing, W., 1981. Excitation functions for $^{182\text{-}186}W(d, 2n)^{182\text{-}186}Re$ and 186W (d, p) 187W reactions. Chin. J. Nucl. Phys. 3, 242.

Ziegler, J.F., Ziegler, M.D., Biersack, J.P., 2010. SRIM—the stopping and range of ions in matter. Nucl. Instrum. Methods Phys. Res. Sect. B 268, 1818–1823.